


# Three-Dimensional Bioprinting of Articular Cartilage: A Systematic Review

CARTILAGE  
2021, Vol. 12(1) 76–92  
© The Author(s) 2018  
Article reuse guidelines:  
sagepub.com/journals-permissions  
DOI: 10.1177/1947603518809410  
journals.sagepub.com/home/CAR  


Yang Wu<sup>1,2\*</sup>, Patrick Kennedy<sup>3\*</sup>, Nicholas Bonazza<sup>3</sup>,  
Yin Yu<sup>4,5</sup>, Aman Dhawan<sup>3</sup>, and Ibrahim Ozbolat<sup>1,2,6,7</sup>

## Abstract

**Objective.** Treatment of chondral injury is clinically challenging. Available chondral repair/regeneration techniques have significant shortcomings. A viable and durable tissue engineering strategy for articular cartilage repair remains an unmet need. Our objective was to systematically evaluate the published data on bioprinted articular cartilage with regards to scaffold-based, scaffold-free and *in situ* cartilage bioprinting. **Design.** We performed a systematic review of studies using the Preferred Reporting Items for Systematic Reviews and Meta-Analyses (PRISMA) guidelines. PubMed and ScienceDirect databases were searched and all articles evaluating the use of 3-dimensional (3D) bioprinting in articular cartilage were included. Inclusion criteria included studies written in or translated to English, published in a peer-reviewed journal, and specifically discussing bioinks and/or bioprinting of living cells related to articular cartilage applications. Review papers, articles in a foreign language, and studies not involving bioprinting of living cells related to articular cartilage applications were excluded. **Results.** Twenty-seven studies for articular cartilage bioprinting were identified that met inclusion and exclusion criteria. The technologies, materials, cell types used in these studies, and the biological and physical properties of the created constructs have been demonstrated. **Conclusion.** These 27 studies have demonstrated 3D bioprinting of articular cartilage to be a tissue engineering strategy that has tremendous potential translational value. The unique abilities of the varied techniques allow replication of mechanical properties and advances toward zonal differentiation. This review demonstrates that bioprinting has great capacity for clinical cartilage reconstruction and future *in vivo* implantation.

## Keywords

bioprinting, articular cartilage, zonal structure, scaffold-free, tissue engineering

## Introduction

Clinical treatment of articular cartilage lesions remains a challenge. Several operative techniques exist for management of appropriate lesions including debridement, fixation, marrow stimulating techniques, cell-based techniques, and osteochondral auto and allografting.<sup>1,2</sup> Despite clinical success obtained with each of these procedures, only osteochondral autograft and allograft recreate the architecture and composition of the native, mature, and architecturally formed articular hyaline cartilage. Osteochondral grafts have limitations particularly with regard to graft availability, donor site morbidity for autograft, and biological risks with allograft. A seminal study has shown that injection of cultured autologous chondrocytes was able to repair articular cartilage defects indicated by the formation of hyaline-like cartilage,<sup>3</sup> and a long-term follow-up study for more than 10 years has indicated that this method was effective and durable for the treatment of large cartilage and osteochondral lesions of the knee joint.<sup>4</sup> However, current clinical restorative technologies, as well as tissue engineering strategies, have been unable to recapitulate the structure of

native hyaline cartilage, which is both heterogeneous and anisotropic, and composed of anatomic zones with specific mechanical and biologic properties.

<sup>1</sup>Engineering Science and Mechanics Department, Penn State University, University Park, PA, USA

<sup>2</sup>The Huck Institutes of the Life Sciences, Penn State University, University Park, PA, USA

<sup>3</sup>Department of Orthopaedics and Rehabilitation, Penn State College of Medicine, Milton S. Hershey Medical Center, Hershey, PA, USA

<sup>4</sup>Institute for Synthetic Biology, Shenzhen Institutes of Advanced Technology, Chinese Academy of Sciences, Shenzhen, People's Republic of China

<sup>5</sup>University of Chinese Academy of Sciences, Beijing, People's Republic of China

<sup>6</sup>Biomedical Engineering Department, Penn State University, University Park, PA, USA

<sup>7</sup>Materials Research Institute, Penn State University, University Park, PA, USA

\*These two authors contributed equally to this work.

## Corresponding Author:

Ibrahim Tarik Ozbolat, Penn State University, W313 Millennium Science Complex, University Park, PA 16802, USA.

Email: ito1@psu.edu

The emergence of 3-dimensional (3D) printing, and specifically 3D bioprinting, presents an opportunity to address numerous tissue engineering (TE) challenges from the ability to print complex tissues using additive manufacturing techniques. This technique has been used for the fabrication of blood vessels, heart, liver, neural tissue, and cartilage.<sup>5,6</sup> The self-assembly and self-organizing capabilities of cells have been delivered through applications of distinct bioprinting techniques (e.g., laser, droplet, and extrusion based).<sup>7-10</sup> Bioprinting may provide a means for implantation of stem cells into host tissue in a very organized and complex manner.<sup>11</sup>

Given the emergence of 3D bioprinting and its possible applications in articular cartilage restoration, we performed a systematic review of the literature to assess (1) the status of research in this emerging field with regard to scaffold-based bioprinting, scaffold-free bioprinting and *in situ* bioprinting and (2) how the existing bioprinted constructs address the current challenges in cartilage TE, specifically with regard to recapitulation of the zonal microarchitecture, mechanical enhancement, cell types and density, and mechanical stimuli. We hypothesized that the collective literature will demonstrate that the morphological, compositional and biomechanical biomimicry of the bioprinted cartilage constructs result in fabricated tissue grafts that demonstrate immunohistologic, microarchitectural, and biomechanical properties that closely resemble hyaline cartilage.

## Selection of Studies

A written protocol was developed in adherence with the Preferred Reporting Items for Systematic Reviews and Meta-Analysis (PRISMA) guidelines to conduct a systematic review of the available literature. PubMed and ScienceDirect electronic databases were searched on June 21, 2018 using the primary search terms “bioprinting” AND “cartilage.” Articles were assessed with the following inclusion criteria: (1) written in or translated to English, (2) published in a peer-reviewed journal, and (3) specifically discussing bioinks and/or bioprinting of living cells related to articular cartilage applications. Review papers, articles in a foreign language, and studies not involving bioprinting of living cells related to articular cartilage applications were excluded. The references of each included article were also cross referenced to ensure that potential studies were not missed.

After the initial search was performed, duplicates were removed from the results of the searches and the titles and abstracts were then screened by the senior authors (AD and IO) and the aforementioned inclusion and exclusion criteria applied. Further screening was performed using the full text of each relevant study if inclusion/exclusion criteria could not be applied by the title and abstract. A diagram of the search methodology can be found in **Figure 1**.

## The State-of-the-Art Techniques for Cartilage Bioprinting

The results of our primary search yielded 360 articles. Removal of duplicates and screening of titles and abstracts with the inclusion and exclusion criteria to include relevance to the study objectives resulted in 50 articles. Further screening of these 50 full text studies with application of inclusion and exclusion criteria resulted in 27 studies that were included in this review and are listed in **Table 1**. We categorized them into 3 sections based on the bioprinting techniques, namely scaffold-based bioprinting, scaffold-free bioprinting, and *in situ* bioprinting. In the cases of scaffold-based bioprinting, studies were further classified into extrusion-based bioprinting (EBB), droplet-based bioprinting (DBB), laser-based bioprinting (LBB), and bioprinting for zonally stratified arrangement.

### Scaffold-Based Bioprinting

Cartilage bioprinting is currently dominated by scaffold-based techniques, and 23 out of the 27 included studies belong to this category.

**Extrusion-Based Bioprinting.** Among scaffold-based approaches, EBB has been the most popular one since its high economic efficiency, ease of operation and flexibility to a wide range of materials.<sup>12,13</sup> EBB takes advantages of automated robotic system for continuous extrusion of bioinks in a filament form, in which pneumatic- or mechanical-driven dispensing systems are mostly employed (**Fig. 2A**). Daly *et al.*<sup>14</sup> evaluated the effects of various bioinks (i.e., agarose, alginate, GelMA, and BioINK) to induce mesenchymal stem cell (MSC)-laden filaments, finding that alginate and agarose bioinks supported more hyaline-like cartilage tissues while gelatin-metacryloyl (GelMA)- and poly(ethylene glycol) methyl ether methacrylate (PEGMA)-based bioinks supported more fibrocartilaginous tissue. With the assistance of polycaprolactone (PCL) filaments, mechanically reinforced scaffold with cell-laden hydrogels was obtained with bulk compressive moduli comparable to articular cartilage (2-3 MPa).

Constantini *et al.*<sup>15</sup> assessed 3 different formulations of hydrogel for scaffold-based bioprinting of cartilage tissue, which were (1) GelMA, (2) GelMA and chondroitin sulfate amino ethyl methacrylate (CS-AEMA), and (3) GelMA, CS-AEMA, and HAMA. Each bioink also contained alginate to aid in stable fiber formation during bioprinting and was loaded with bone marrow-derived MSCs (BM-MSCs) (**Fig. 2B**). The bioink composed of alginate, GelMA, and CS-AEMA has been observed to be the best in chondrogenic formation with the highest COL-II versus COL-I and COL-X ratios. The deposition method also showed maintained shape fidelity with a layer thickness of 100  $\mu\text{m}$  and interfiber distance of 300  $\mu\text{m}$ .

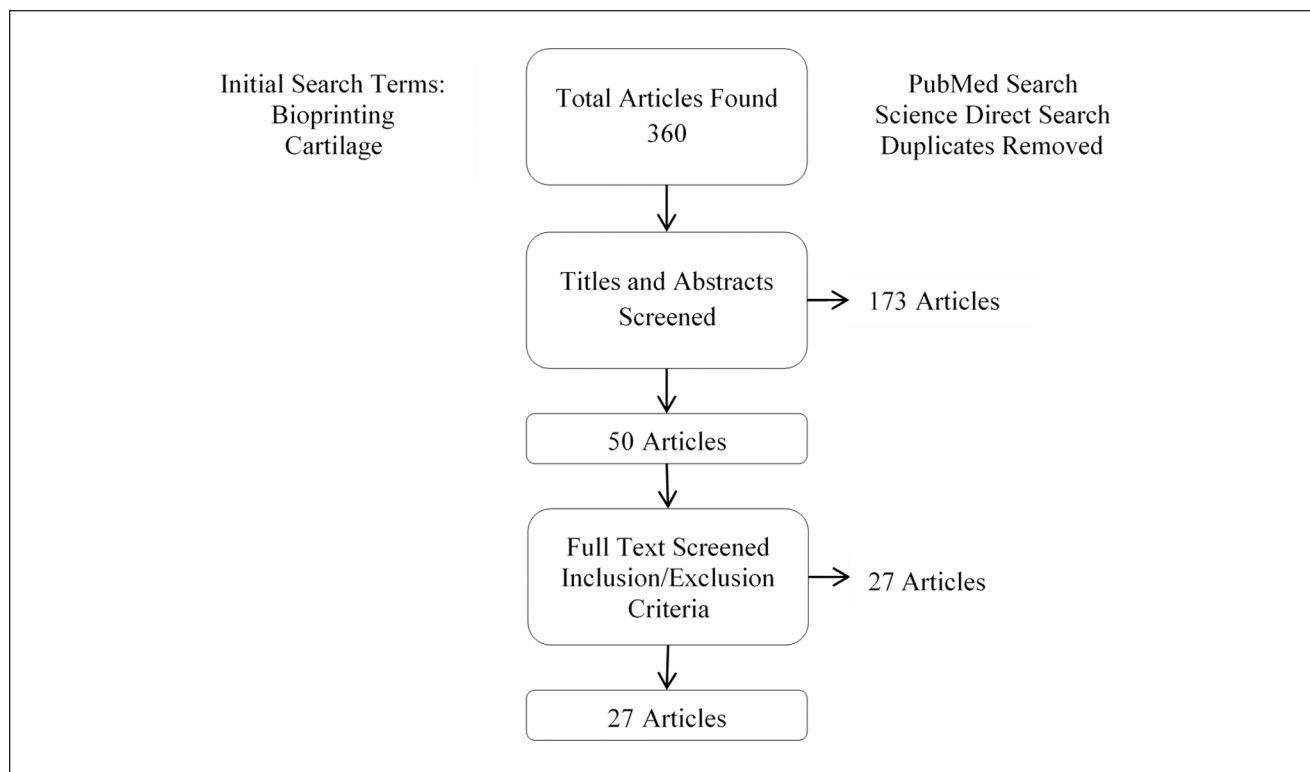


**Figure 1.** Search methodology for selection of studies.

In a more recent study, Mouser *et al.*<sup>16</sup> investigated the effect of gellan gum (GG) on GelMA bioink systemically. Various concentrations (i.e., 3%-20% GelMA with 0%-1.5% GG) were evaluated to define a bioprinting window. They found a concentration of 10/0.5% GelMA/GG balanced the bioprintability and construct stiffness that impacted cell incorporation. From the same research group, Abbadessa *et al.*<sup>17</sup> designed a hydrogel system based on triblock copolymers of polyethylene glycol (PEG, 10 kDa in molecular weight) and poly(*N*-(2-hydroxypropyl) methacrylamide mono/dilactate) (i.e., polyHPMA-lac-PEG) with degree of methacrylation of 15%, as bioink (i.e.,  $M_{15}P_{10}$ ) for cartilage bioprinting. With the mixture of methacrylated chondroitin sulfate (CSMA),  $M_{15}P_{10}$  exhibited superior mechanical and thermal properties compared to  $M_{15}P_{10}$  alone, and was able to maintain cell viability of embedded chondrogenic ATDC5 cells for 6 days in a preliminary *in vitro* test. In a follow-up study, Abbadessa *et al.*<sup>18</sup> blended the  $M_{10}P_{10}$  with methacrylated polysaccharides including chondroitin sulfate (CS) or hyaluronic acid (HAMA) (Fig. 2C). The bioink with incorporation of polysaccharides exhibited increased storage modulus and decreased degradation kinetics in crosslinked hydrogels, while the inclusion of HAMA improved printability versus  $M_{10}P_{10}$  and yielded in 3D constructs with excellent cell viability (>90%) of equine chondrocytes at 42 days of culture. Most recently, they further explored the printability of polyHPMA-lac-PEG with HAMA to optimize

cartilage-like tissue formation by embedded chondrocytes.<sup>19</sup> On being seeded with equine chondrocytes, it has been found that intermediate HAMA concentrations (0.25%-0.5%) increased cartilage-like matrix production including collagen type II (COL-II), VI and IV, and sulphated glycosaminoglycans (GAG) compared to HAMA-free hydrogels, while higher concentrations (~1%) resulted in undesirable fibrocartilage formation with the presence of collagen type I (COL-I). Similar to Daly's study, PCL was incorporated with the hydrogels in various construct designs in order to obtain mechanical reinforcement, with Young's moduli ranging from 3.5 and 4.6 MPa.

To exploit the cellulose in terms of mechanical strength and rheology, Markstedt *et al.*<sup>20</sup> evaluated the printability and cytotoxicity of nanofibrillated cellulose (NFC) and alginate bioink (Fig. 2D). The combination was utilized due to favorable shear thinning properties of the NFC with the fast crosslinking ability of alginate. Specifically, with regard to articular cartilage, human chondrocytes were bioprinted using this noncytotoxic bioink in gridded constructs. Viability was demonstrated at 86% after seven days of culture. Successful mixing of the cells in the bioink was also shown via a homogenous cell distribution. Decrease in cell viability was observed, which was attributed to the shear stress in the mixing process. In another study, Nguyen *et al.*<sup>21</sup> compared NFC/alginate and NFC/hyaluronic acid (NFC/HA) composites for cartilage bioprinting. Human-derived

**Table 1.** Summaries of the Technologies and Properties of the Bioprinted Constructs for Cartilage Tissue Engineering.

	Study	Materials	Cell Source	Animal Model	Mechanical Reinforcement	Compressive Modulus	Zonal Structure	In Vitro	In Vivo
Scaffold-based bioprinting (EBB)	Daly et al. (2016)	Agarose, alginate, GelMA, and PEGMA	MSC	—	Extruded PCL fibers	Without PCL: <40 kPa, with PCL: ~2-3 MPa	—	<ul style="list-style-type: none"> <li>MSC-laden alginate hydrogels stained intensely for sulfated GAG and COL-II. GelMA and PEGMA stained stronger for COL-I</li> <li>High levels of cell viability were observed in all bioinks postprinting</li> <li>Alginate and agarose hydrogels best supported the development of hyaline-like cartilage, and GelMA and PEGMA supported the development of a more fibrocartilage-like tissue.</li> </ul>	—
	Markstedt et al. (2015)	NFC and alginate	hNC	—	—	~35 kPa	—	<ul style="list-style-type: none"> <li>Cell viability was 73% and 86% after 1 and 7 days of printing.</li> </ul>	—
	Nguyen et al. (2017)	NFC, alginate and HA	iPSCs and chondrocytes	—	—	—	—	<ul style="list-style-type: none"> <li>Low proliferation and phenotypic changes away from pluripotency were seen in NFC/HA.</li> <li>In 3D-bioprinted NFC/HA constructs, pluripotency was initially maintained, and hyaline-like cartilaginous tissue with COL-II expression and lacking tumorigenic Oct4 expression was observed after 5 weeks.</li> <li>A marked increase in cell number within the cartilaginous tissue was detected.</li> </ul>	—
	Mouser et al. (2016)	GelMa-GG	Primary equine chondrocytes	—	—	~3-200 kPa	—	<ul style="list-style-type: none"> <li>The addition of GG supported chondrogenesis, evidenced by presence of GAGs.</li> <li>High GG concentrations compromised cartilage matrix production and distribution, and even higher concentrations resulted in cell encapsulation.</li> </ul>	—
	Abbadessa et al. (2016)	M <sub>15</sub> P <sub>10</sub> and CSMA	ATDC5 cells	—	—	~8-60 kPa	—	<ul style="list-style-type: none"> <li>Embedded cells remained viable and proliferating over a culture period of 6 days.</li> </ul>	—
	Abbadessa et al. (2016)	M <sub>10</sub> P <sub>05</sub> CSMA and HAMA	Primary equine chondrocytes	—	—	~15 kPa	—	<ul style="list-style-type: none"> <li>The cell-laden hydrogel supported expression of proteoglycans, COL-II and VI for 42 days culture.</li> </ul>	—
	Mouser et al. (2017)	polyHPMA-lac-PEG, HAMA, and PCL	Primary equine chondrocytes	—	Extruded PCL fibers	Without PCL: ~15-30 kPa, with PCL: ~4-8 MPa	—	<ul style="list-style-type: none"> <li>GAG and COL-II content increased with HAMA concentrations (0.25%-0.5%) compared with HAMA-free hydrogels</li> <li>A relatively high HAMA concentration (1%) resulted in increased fibrocartilage formation.</li> <li>The polyHPMA-lac-PEG hydrogels with 0.5% HAMA was optimal for cartilage-like tissue formation.</li> </ul>	—

(continued)

Table 1. (continued)

Study	Materials	Cell Source	Animal Model	Mechanical Reinforcement	Compressive Modulus	Zonal Structure	In Vitro	In Vivo
Constantini et al. (2016)	GelMA, CS-AEMA, and HAMA	BM-MSCs	—	—	~50-100 kPa	—	<ul style="list-style-type: none"> <li>Cell viability was ~90% for all the hydrogels</li> <li>Hydrogel with alginate, GelMA, and CS-AEMA was the best candidate in neocartilage formation with the highest COL-II/COL-I and COL-III/COL-X ratios.</li> <li>Addition of HAMA favored the differentiation toward hypertrophic cartilage.</li> </ul>	—
Kundu et al. (2015)	PCL and alginate	Human chondrocytes	Mouse	Extruded PCL fibers	—	—	<ul style="list-style-type: none"> <li>PCL-alginate gels with TGF<math>\beta</math> showed higher ECM formation (GAG and total collagen content).</li> </ul>	<ul style="list-style-type: none"> <li>Implants after 4 weeks revealed enhanced cartilage tissue (GAG) and COL-II fibril formation in the PCL-alginate gel with TGF<math>\beta</math></li> </ul>
Izadifar et al. (2016)	PCL and alginate	Embryonic chick chondrocytes and ATDC5 cell line	—	Extruded PCL fibers	—	—	<ul style="list-style-type: none"> <li>Rounded cells had higher COL-II mRNA levels than the fibroblastic cells, while fibroblastic cells had higher COL-II mRNA levels than the rounded cells after biofabrication</li> <li>Rounded and fibroblastic cells demonstrated high viability in hybrid constructs</li> <li>Fibroblastic cells had higher proliferation than rounded</li> <li>Fibroblastic cells produced more Alcian blue-stained matrix than the rounded cells</li> </ul>	—
Olubamiji et al. (2017)	PCL and alginate	ATDC5 cell line	Mouse	Extruded PCL fibers	—	—	<ul style="list-style-type: none"> <li>Cells within the cartilage constructs remained viable over 21 days postimplantation.</li> <li>Progressive secretion of cartilage matrix in implanted cartilage constructs (sulfated GAG and COLII) over 21 days</li> <li>SR-inline-PCL-CT enabled noninvasive visualization of the individual components of cartilage constructs, surrounding host tissues and their structural changes postimplantation.</li> </ul>	—
Yang et al. (2018)	COL-I, agarose and alginate	Rat primary chondrocytes	—	—	~25-70 kPa	—	<ul style="list-style-type: none"> <li>SA/COL facilitated cell adhesion, accelerated cell proliferation and enhanced the expression of cartilage specific genes (Aggrecan, COL-II, and Sox9).</li> <li>Lower expression of COL-I was present in SA/COL group than SA and SA/AG groups, indicating that SA/COL suppressed dedifferentiation of chondrocytes and preserved the phenotype.</li> </ul>	—

(continued)

**Table 1. (continued)**

Study	Materials	Cell Source	Animal Model	Mechanical Reinforcement	Compressive Modulus	Zonal Structure	In Vitro	In Vivo
Scaffold-based bioprinting (DBB)								
Cui et al. (2012)	PEGDMA	Human articular chondrocytes	—	—	~40-90 kPa	—	<ul style="list-style-type: none"> <li>The presence of TGFβ1 is essential for the induction or maintenance of the chondrocyte phenotype (COL-II and aggrecan).</li> <li>Pre-culture or co-culture with FGF-2 to stimulate cell proliferation does not interfere with the chondrogenic effect of TGF-β1.</li> <li>FGF-2/TGF-β1 treated constructs showed overall higher amount of proteoglycan content</li> <li>ECM production per chondrocyte in low cell density was much higher than that in high cell seeding density.</li> </ul>	—
Cui et al. (2012)	PEGDMA	Human articular chondrocytes	—	—	~300-500 kPa	—	<ul style="list-style-type: none"> <li>Viability of printed chondrocytes increased 26% in simultaneous polymerization than polymerized after printing.</li> <li>Printed construct attached firmly with surrounding tissue and showed greater proteoglycan deposition at the interface of implant and native cartilage.</li> <li>Printed cartilage in 3D OC plugs had elevated GAG content comparing to that without OC plugs.</li> </ul>	—
Gao et al. (2015)	PEGDMA and GelMA	BM-MSCs	—	—	~40-60 kPa	—	<ul style="list-style-type: none"> <li>The procedure showed a good biocompatibility</li> <li>Gene expression analysis showed both osteogenic and chondrogenic differentiation was improved by PEG-GelMA in comparison with PEG alone.</li> </ul>	—
Gao et al. (2015)	Peptide-conjugated PEG	BM-MSCs	—	—	~30-70 kPa	—	<ul style="list-style-type: none"> <li>Cell viability of &gt;85%</li> <li>The bioprinted bone and cartilage tissue demonstrated excellent mineral and cartilage matrix deposition with osteogenic and chondrogenic differentiation</li> <li>Bioprinted PEG-peptide scaffold inhibited hMSC hypertrophy during chondrogenic differentiation</li> </ul>	—
Gao et al. (2017)	PEGDA	BM-MSCs	Mouse	—	~75-100 kPa	—	<ul style="list-style-type: none"> <li>NR2F2 overexpressed MSCs showed significantly enhanced chondrogenesis in monolayer, 3D pellet, and hypoxia cultures</li> <li>More proteoglycan deposition was found in scaffold using NR2F2 overexpressed cells comparing with the control group.</li> </ul>	<ul style="list-style-type: none"> <li>Vascularized tissue membrane was formed surrounding the constructs</li> <li>Dense and well-organized collagen formation, GAG and COL-II production were observed after 8 weeks of implantation</li> </ul>
Xu et al. (2013)	Collagen, fibrinogen and PCL	Rabbit articular chondrocytes	Mouse	Electrospun PCL fibers	~1.8 MPa	Alternant hydrogel and electrospun layers	<ul style="list-style-type: none"> <li>Cell viability &gt;80% one week after printing</li> <li>Constructs formed cartilage-like tissues as evidenced by the deposition of COL-II and GAG</li> </ul>	

(continued)

**Table 1. (continued)**

Study	Materials	Cell Source	Animal Model	Mechanical Reinforcement	Compressive Modulus	Zonal Structure	<i>In Vitro</i>	<i>In Vivo</i>
Scaffold-based bioprinting (LBB)	Zhu <i>et al.</i> (2018)	BM-MSCs	—	—	~1-18 MPa	—	<ul style="list-style-type: none"> <li>Cells grown on 5%/10% (PEGDA/GelMA) hydrogel present the highest cell viability and proliferation rate.</li> <li>The TGF-<math>\beta</math>1 embedded in nanospheres can keep a sustained release up to 21 d and improve chondrogenic differentiation.</li> </ul>	—
Scaffold-based bioprinting (zonally stratified arrangement)	Levato <i>et al.</i> (2014)	MSC	—	PLA microcarriers	~30-50 kPa	Cartilage region and bone region	<ul style="list-style-type: none"> <li>Microcarrier encapsulation facilitated cell adhesion and supported osteogenic differentiation and bone matrix deposition by MSCs.</li> <li>Microcarrier-cell complexes displayed a high viability after the automated printing process</li> </ul>	—
	Levato <i>et al.</i> (2017)	ACPCs, MSCs and chondrocytes	—	—	~100-190 kPa	ACPC-laden and MSC-laden zones	<ul style="list-style-type: none"> <li>ACPCs outperformed chondrocytes in terms of sulphated GAG</li> <li>MSCs produced significantly more sulphated GAG and had higher gene expression of COL-II and aggrecan than both ACPCs and chondrocytes.</li> <li>ACPCs had the lowest gene expression levels of COL-X, and the highest expression of PRG4</li> <li>MSC/ACPC co-cultured matrices displayed the highest overall sulphated GAG concentration than MSC/chondrocytes and ACPC/chondrocytes.</li> <li>In bioprinted zonal-like constructs, different distributions of sulphated GAG, COL-I and II were observed in ACPC- and MSC-laden zones</li> </ul>	—
	Ren <i>et al.</i> (2016)	Chondrocytes from New Zealand white rabbits	—	—	—	Cell density gradient	<ul style="list-style-type: none"> <li>Gradient cell distribution patterns were established and maintained</li> <li>Cell viability was &gt;90%</li> <li>GAG content was positively correlated with the total cell density</li> <li>Cellular biosynthetic ability was affected by both the total cell density and the cell distribution pattern.</li> </ul>	—
	Shim <i>et al.</i> (2016)	Human mesenchymal stromal cells	Rabbits	Extruded PCL fibers	—	Subchondral bone layer and superficial cartilage layer	<ul style="list-style-type: none"> <li>Cell viability was ~90%</li> <li>The cells in the atelocollagen hydrogel layer exhibited increases in ALP, COL-I, and OSX genes</li> <li>The cells in the CB[6]/DAH-HA hydrogel exhibited increases in ACAN, COL-II, and SOX9 genes</li> <li>Cells in atelocollagen showed Runx2 expression and calcium deposition, and cells cultured in CB[6]/DAH-HA showed COL-II and GAG deposition.</li> </ul>	<ul style="list-style-type: none"> <li>The defect treated by layered scaffold was covered with neotissue without fiber exposure and exhibited a smooth surface.</li> <li>Layered scaffold showed a remarkable capability for the osteochondral regeneration at week 8. The newly regenerated cartilage tissues were smoothly integrated with ends of the host cartilage tissue.</li> <li>GAG, COL-II and X were strongly expressed in only layered scaffold.</li> </ul>

(continued)

**Table 1. (continued)**

	Study	Materials	Cell Source	Animal Model	Mechanical Reinforcement	Compressive Modulus	Zonal Structure	<i>In Vitro</i>	<i>In Vivo</i>
Scaffold-free bioprinting	Yu <i>et al.</i> (2016)	Cell ink	Primary cattle chondrocytes	—	—	~1.5 MPa	—	<ul style="list-style-type: none"> <li>Cell viability in strands was &gt; 85%</li> <li>Tissue strands showed slightly higher proteoglycan production than native cartilage, and significant amount of COL II and aggrecan</li> <li>Printed tissue also had a significant amount of proteoglycan formation and the interface of each tissue strand was well integrated.</li> <li>High sulfated GAG content and cell density, and chondrocytes with rounded morphology were observed in printed construct</li> <li>In a bovine osteochondral model, the explants tissue adhered to the defect, stayed intact and exhibited proteoglycan-rich ECM.</li> <li>Cell viability was &gt;97%</li> </ul>	—
<i>In situ</i> bioprinting	O'Connell <i>et al.</i> (2016) Duchi <i>et al.</i> (2017)	GelMA/HAMA	Human infrapatellar fat pad derived adipose stem cells Sheep ADSCs	—	—	~9.380 kPa	—	<ul style="list-style-type: none"> <li>UV light exposure at 700 mW/cm<sup>2</sup> did not significantly affect cell viability compared with the untreated cells</li> <li>Cells printed by coaxial configuration were observed to retain viability and proliferative capability</li> <li>The mono-axial bioprinting configuration shows a viability decrease by 30% compared with coaxial printing.</li> </ul>	—
	Di Bella <i>et al.</i> (2017)	GelMA/HAMA	Sheep MSCs	Sheep	—	~0.5 MPa	—	<ul style="list-style-type: none"> <li>There was better overall macroscopic appearance in the handheld printed group compared with control groups.</li> <li>Handheld printed construct showed a higher amount of newly regenerated cartilage with chondrocytes columnar alignment, and the absence of subchondral bone deformation or collapse</li> <li>Handheld printed construct showed positive Safranin O and COL-II staining.</li> </ul>	—

Note: GelMA = gelatin-methacryloyl; PEGMA = poly(ethylene glycol) methyl ether methacrylate; MSC = mesenchymal stem cell; PCL = polycaprolactone; GAG = glycosaminoglycans; COL-I, II, VI and X = collagen types; NFC = nanofibrillated cellulose; hNC = human nasoseptal chondrocytes; HA = hyaluronic acid; iPSCs = induced pluripotent stem cells; NFC/A = nanofibrillated cellulose/alginate; GG = gellan gum; CSMA = methacrylated chondroitin sulfate; HAMA = methacrylated hyaluronic acid; PEG = polyethylene glycol; CS-AEMA = chondroitin sulfate amino ethyl methacrylate; BM-MSCs = bone marrow-derived mesenchymal stem cells; TGF-β = transforming growth factor-β; ECM = extracellular matrix; SR-inline-PCI-CT = synchrotron radiation inline phase contrast imaging computed tomography; SA = sodium alginate; AG = agarose; PEGDMA = poly(ethylene glycol) dimethacrylate; FGF-2 = fibroblast growth factor-2; OC = osteochondral; PEGDA = polyethylene glycol diacrylate; NR2F2 = nuclear receptor subfamily 2 group F member 2; PLGA = poly(lactic-co-glycolic acid); PLA = polylactic acid; ACPs = articular cartilage-resident chondroprogenitor cells; PRG4 = proteoglycan 4; ALP = alkaline phosphatase; Osx = osterix; CB[6]-HA = cucurbit[6]uril-conjugated hyaluronic acid; ACAN = aggrecan; Runx2 = runt-related transcription factor 2; ADSCs = adipose-derived stem cells; UV = ultraviolet.



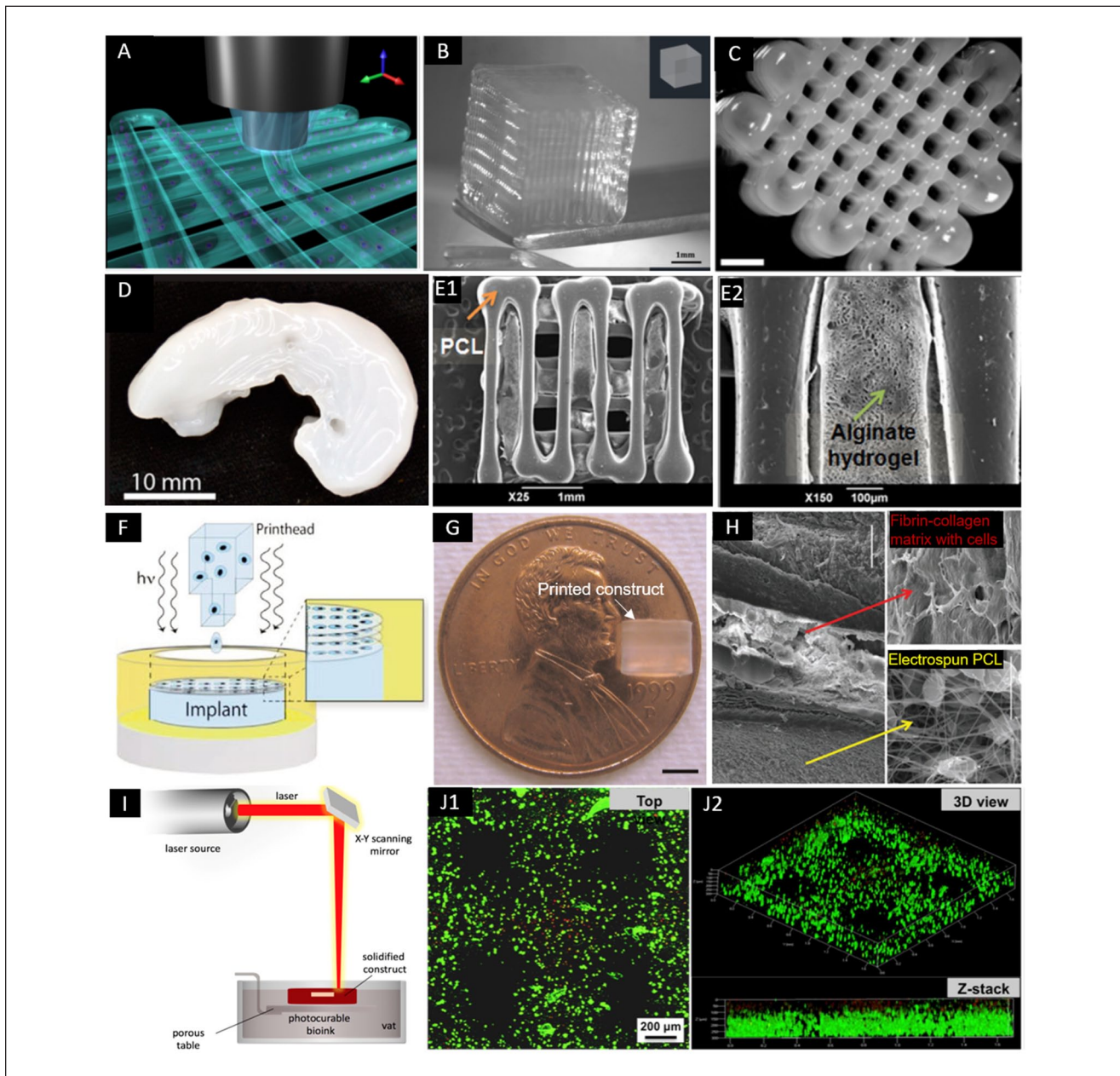


**Figure 2.** Bioprinted constructs using EBB, DBB, and LBB. **(A)** Three-dimensional illustration of hydrogel fibers deposition in EBB (adapted with permission from [ref 15]).<sup>15</sup> **(B)** Three-dimensional printed construct using alginate with GelMA (adapted with permission from [ref 15]).<sup>15</sup> **(C)** Three-dimensional printed porous constructs based on  $M_{10}P_{10}$  blended with HAMA (adapted with permission from [ref 17]).<sup>17</sup> **(D)** Three-dimensional printed sheep meniscus with bioink of nanofibrillated cellulose and alginate (scale bar = 2 mm) (adapted with permission from [ref 20]).<sup>20</sup> **(E)** Three-dimensional bioprinted hybrid constructs with PCL supporting structure and the cell-laden alginate hydrogel (adapted with permission from [ref 22]).<sup>22</sup> **(F)** A schematic of DBB with simultaneous photopolymerization process (adapted with permission from [ref 27]).<sup>27</sup> **(G)** A printed PEG hydrogel construct with 4 mm in diameter and 4 mm in height (scale bar = 2 mm) (adapted with permission from [ref 27]).<sup>27</sup> **(H)** Multiple-layered printed construct which was composed of layers of electrospun PCL fibers and layers of cell-laden fibrin-collagen matrix printed by DBB (scale bar = 100  $\mu\text{m}$ ) (adapted with permission from [ref 31]).<sup>31</sup> **(I)** A schematic illustration of LBB for cartilage (adapted from [ref 68]).<sup>68</sup> **(J)** Live-dead staining of MSCs within 5% PEGDA/GelMA bioprinted construct after culturing (adapted with permission from [ref 32]).<sup>32</sup> EBB = extrusion-based bioprinting; DBB = droplet-based bioprinting; LBB = laser-based bioprinting; MSCs = mesenchymal stem cells; GelMA = gelatin-methacryloyl methacrylate; PEGMA = poly(ethylene glycol) methyl ether methacrylate; HAMA = hyaluronic acid methacrylate; PCL = polycaprolactone.

induced pluripotent stem cells (iPSCs) were co-printed with irradiated human chondrocytes, and low proliferation and phenotypic changes away from pluripotency were seen in NFC/HA bioink. On the contrary, pluripotency in the bioprinted NFC/alginate constructs was maintained, and hyaline-like cartilaginous tissue with COL-II expression was observed without any presence of tumorigenic Oct4 expression. Moreover, a remarkable increase in cell number within the cartilaginous tissue was detected in co-cultured constructs.

Kundu *et al.*<sup>22</sup> used a layer-by-layer deposition of PCL and chondrocyte-laden alginate hydrogel (**Fig. 2E**). The *in vitro* assessment indicated that the structure of 4% alginate with the addition of transforming growth factor- $\beta$  (TGF- $\beta$ ) produced more GAG, DNA and cartilaginous extracellular matrix (ECM) than those of other groups. In a mouse model, scaffolds with the addition of TGF- $\beta$  also resulted in more cartilage formation and COL-II fibril after 4 weeks of implantation, without any adverse tissue response.

Izadifar *et al.*<sup>23</sup> cultured 2 distinct cell populations from embryonic chick cartilage (i.e., rounded and fibroblastic), and have elucidated that printed hybrid constructs of melted PCL and cell-impregnated alginate with fibroblastic cells showing higher cell numbers than the rounded cells at 14 days. Rounded cells had a significantly higher expression of COL-II, while fibroblastic cells expressed significantly higher levels of COL-I and GAG matrix. A scale-up printing has also been performed using the ATDC5 chondrogenic cell line to create six-layer constructs which demonstrated good biofunctionality. In their *in vivo* study,<sup>24</sup> bioprinted cartilage constructs with ATDC5 cells were implanted subcutaneously in mice over 21 days. The implants were characterized both non-invasively using a synchrotron radiation inline phase contrast imaging computed tomography (SR-inline-PCI-CT) approach and invasively to evaluate their cell viability (>70%) and secretion of cartilage-specific ECM. Secretion of GAG and COL-II increased progressively over time. Also, SR-inline-PCI-CT enabled visualization of the individual components of the 3D printed hybrid constructs (PCL and hydrogel), their time-dependent structural changes after implantation and their connection to surrounding host tissues *in situ*.

In another recently published study, Yang *et al.*<sup>25</sup> mixed COL-I or agarose (AG) with sodium alginate (SA) as bioinks. The *in vitro* results using chondrocytes showed that the mechanical strength was improved in both SA/COL and SA/AG groups compared with SA alone. Among the 3 scaffolds, SA/COL could distinctly facilitate cell adhesion, accelerated cell proliferation and enhanced the expression of cartilage specific genes such as aggrecan, COL-II and Sox9 than the other two groups. Lower expression of COL-I was present in SA/COL group than that in both of SA and SA/AG groups. The results indicated that SA/COL

effectively suppressed dedifferentiation of chondrocytes and preserved the phenotype.

**Droplet-Based Bioprinting.** In DBB, the bioink made up of living cells and other biological materials (e.g., hydrogels) is deposited in a droplet form with precise noncontact positioning (**Fig. 2F**).<sup>12</sup> The droplets are generated by one of thermal, piezoelectric, or electrostatic drop-on-demand technologies. For cartilage TE applications, Cui *et al.*<sup>26</sup> have demonstrated the bioprinting with thermal inkjet-based technology utilizing a bioink composed of Poly(ethylene glycol) dimethacrylate (PEGDMA)-laden with human chondrocytes along with the addition of fibroblast growth factor-2 (FGF-2) and/or TGF- $\beta$ 1 (**Fig. 2G**) and found that the cell proliferation and chondrocyte phenotype were optimized with a combination of the factors versus TGF- $\beta$ 1 only group. In another study, Cui *et al.*<sup>27</sup> used the same technique and materials to repair defects in osteochondral plugs. The printed construct exhibited the compressive modulus of 0.4 MPa, and bioprinted human chondrocytes were able to maintain the initial positions due to simultaneous photopolymerization of surrounded biomaterial. In an *in vitro* implantation using an osteochondral plug, the printed cartilage implant obtained a firm attachment with surrounding tissue, and greater proteoglycan deposition was observed at the interface of implant and native cartilage. In the follow-up studies from the same group, Gao *et al.*<sup>28,29</sup> extended the cell source to MSC and added other components (e.g., peptide or GelMA) to optimize MSC differentiation. Their results showed successful printing of a layered structure that developed a higher modulus than PEG scaffolds after osteogenic and chondrogenic differentiation, which was also improved over PEG alone evidenced by gene and protein expression analysis.

In a mouse model, Gao *et al.*<sup>30</sup> implanted bioprinted constructs with nuclear receptor subfamily 2 group F member 2 (NR2F2) overexpressed MSCs for 21 days. Vascularized tissue membranes were found to grow around the implanted constructs *in vivo*. The compressive modulus of scaffolds with NR2F2 were significantly stiffer than controls with more proteoglycan growth. Observations among gene expression, biochemical analysis, histological assay, and biomechanical evaluation were consistent to indicate that NR2F2 over-expressed MSCs had enhanced chondrogenic potential for cartilage regeneration.

By combining inkjet printing and electrospinning techniques, Xu *et al.*<sup>31</sup> created 5-layered constructs that consisted of alternating layers of electrospun PCL/F-127 fibers (3 layers) and inkjet-printed chondrocytes/fibrin/collagen hydrogel (2 layers) (**Fig. 2H**). After culturing *in vitro* for 2 weeks, the hybrid constructs were implanted in mice subcutaneously for 8 weeks. The chondrocytes showed > 80% viability one week after printing. The fabricated constructs formed cartilage-like tissues both *in vitro* and *in vivo* as

evidenced by the deposition of type II collagen and GAG. Moreover, the bioprinted hybrid scaffolds demonstrated enhanced mechanical properties compared to printed alginate or fibrin/collagen gels alone.

**Laser-Based Bioprinting.** LBB was operated based on the principle of a laser energy beam used for precise patterning of biomaterials.<sup>12</sup> Laser energy can be used in 2 different modalities, one of which involves photopolymerization (e.g., stereolithography or 2-photon polymerization) (**Fig. 2I**), and the other modality is based on cell transfer (e.g. laser guided direct writing and laser induced forward transfer). As the only one study using LBB for cartilage TE, Zhu *et al.*<sup>32</sup> have reported the utilization of a tabletop stereolithography-based bioprinter for cell-laden cartilage fabrication very recently. The bioresin was composed of 10% GelMA base, various concentrations of polyethylene glycol diacrylate (PEGDA), a biocompatible photoinitiator, and TGF- $\beta$ 1 embedded nanospheres fabricated by the electrospraying technique, and MSCs were then mixed with the resin at density of  $2 \times 10^6$  cells/mL. The addition of PEGDA into GelMA hydrogel greatly improved the printing resolution and modulus of the bioprinted scaffolds as compared with GelMA only. Importantly, cell viability and the bioactivity of growth factors were maintained after UV photopolymerization. TGF- $\beta$ 1 embedded in nanospheres kept a sustained release up to 21 days and improved the chondrogenic differentiation of encapsulated MSCs (**Fig. 2J**).

**Bioprinting for Zonally Stratified Arrangement.** To generate a bilayered osteochondral model, Levato *et al.*<sup>33</sup> used microcarriers of polylactic acid (PLA) to load MSCs via static culture or spinner flask expansion, followed by encapsulating the cell-laden microcarriers in GelMA/GG. The cartilage region was printed with GelMA-GG and the bone region was represented by GelMA-GG with encapsulated microcarriers. The application of microcarriers allowed for extensive expansion of cells within the hydrogel, resulting in a higher compressive modulus of the construct and improved cell adhesion. In 2017, Levato *et al.*<sup>34</sup> reported another strategy for zonal-like structure fabrication using a recently identified articular cartilage-resident chondroprogenitor cells (ACPCs). GelMA-based hydrogels were used to culture ACPCs, MSCs and chondrocytes as bioinks, in which ACPCs outperformed chondrocytes in terms of neo-cartilage production. Even though ACPC-laden hydrogels showed a lower production of ECM components compared with MSC-laden ones, ACPCs displayed a low expression of COL-X and a high expression of proteoglycan 4 (PRG4), suggesting a phenotype similar to superficial zone of cartilage. By bioprinting ACPC- and MSC-laden bioinks with a density of  $2 \times$

$10^7$  and Pluronic as a sacrificial ink, a bioprinted model of articular cartilage was generated, consisting of defined superficial and deep regions with distinct cellular and ECM composition (**Fig. 3A**).

Ren *et al.*<sup>35</sup> used bioprinted COL-II hydrogel scaffolds to create a biomimetic cell density gradient. A construct with a 6-mm height and a 4-mm radius was bioprinted containing three layers (deep, middle, and superficial zones) with cell density gradient to imitate distribution of cell densities in native cartilage. The gradient in cell density resulted in a gradient of ECM, which further affected the biosynthetic ability of the chondrocytes.

Targeting at reconstruction of an osteochondral tissue in the knee joint, Shim *et al.*<sup>36</sup> used PCL as supporting for multilayered hydrogel extrusion with human MSCs. The construct (5 mm in height) was divided into 2 distinct layers, which were subchondral bone layer printed using atelocollagen with MSCs and recombinant human bone morphogenic protein (rhBMP)-2, and superficial cartilage layer comprised of Cucurbit[6]uril-conjugated hyaluronic acid (CB[6]-HA), 1,6-diaminohexane-conjugated HA (DAH-HA), MSCs and TGF- $\beta$ . Cell viability of  $\sim 90\%$  were observed in both layers with increased proliferation over time. The cells in the CB[6]/DAH-HA hydrogel exhibited upregulation in the expression of cartilage-related genes (aggrecan, COL-II, and SOX9) and deposition of GAG compared with those in the atelocollagen hydrogel layer, whereas atelocollagen hydrogels showed strong calcium deposition. Through implanting the bioprinted scaffold into New Zealand white rabbit knee joints, the newly regenerated cartilage tissues were smoothly integrated with ends of the host cartilage tissue at 8 weeks of implantation. They also found the lacuna structure to be similar to that of native cartilage. Immunochemical analysis also showed zonal cartilage regeneration, although COL-X was seen in the superficial layer which is abnormal in comparison to normal cartilage.

### Scaffold-Free Bioprinting

Among these studies, only one pioneer study has evaluated scaffold-free bioprinting of articular cartilage. Yu *et al.*<sup>37</sup> fabricated tissue strands of bovine chondrocytes by spinning the cells down into a cell mass, and then transferred them into an alginate capsules for incubation (**Fig. 3B**). Using an extrusion apparatus, the tissue strands were able to be directly bioprinted while maintaining the shape in culture. The printed construct maintained their fidelity for 10 days, with the observation of ECM deposition and cell-cell adhesion. Mechanical strength of the strands also exhibited increase from 28 kPa at 1 week to 3.4 MPa at 3 weeks for ultimate strength, and from 1 MPa to 5.3 MPa for the Young's modulus, which approached the native values.

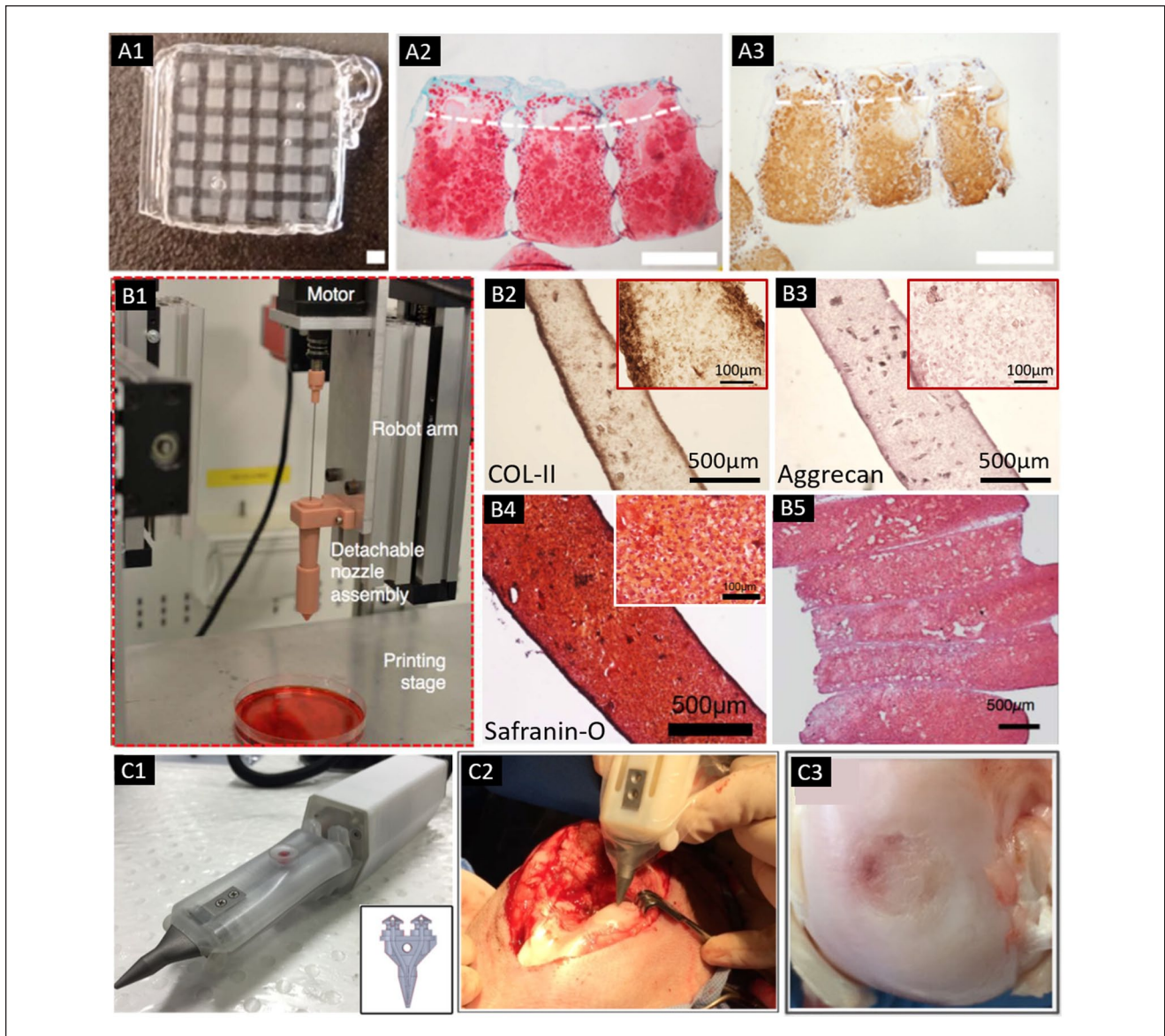


**Figure 3.** (A) Bioprinted cartilage constructs with the Pluronic frame (A1), which was bioprinted with MSCs in the middle/deep layer and ACPCs in the superficial layer. Histological staining after 56 days of culture for (A2) sulfated GAGs and (A3) collagen type II (scale bar = 1 mm) (adapted with permission from [ref 34]).<sup>34</sup> (B) Bioprinting setup with detachable nozzle assembly for tissue strand bioprinting (B1). Positive COL II (B2), aggrecan (B3), and safranin-O staining (B4) was obtained in tissue strands. (B5) A bioprinted cartilage tissue patch showed sulphated GAG deposition throughout the entire construct (adapted from [ref 37]).<sup>37</sup> (C) The biopen with 2 separate chambers. Insert showed that 2 chambers are connected to the printing nozzle (insert), which allows the coaxial printing of the 2 different bioinks in a core/shell distribution (C1). (C2) Intraoperative bioprinting using the biopen for treatment of a full-thickness chondral defect in a sheep. (C3) Macroscopic appearance of the treated defect at 8 weeks after implantation (adapted with permission from [ref 40]).<sup>40</sup>

Chondrocyte phenotype maintained evidenced by expression of COL-II and aggrecan markers and the upregulated COL-II and aggrecan gene expression. Multilayer tissue strands were able to be 3D bioprinted into tight layers and ultimately fused into a single unit as early as 12 hours after incubation. Implanted tissue into *in vitro* defects also demonstrated proteoglycan rich ECM at 4 weeks.

### *In Situ* Bioprinting

Among the included studies, a promising handheld device has been developed for *in situ* cartilage repair. O’Connell *et al.*<sup>38</sup> aimed to translate freeform biofabrication into the surgical field, and hence come up with a handheld biofabrication tool, named the “biopen,” in which GelMA/HAMA

hydrogel was manually extruded and ultraviolet (UV) crosslinked during the deposition process to generate surgically sculpted 3D structures (Fig. 3C). To progress toward translating this technique into clinical practice, Duchi *et al.*<sup>39</sup> further determined the ideal bioprinting conditions, which allowed the generation of core/shell GelMA/HAMA scaffolds with stiffness of 200 kPa, obtained after 10 seconds of exposure to 700 mW/cm<sup>2</sup> of 365 nm UV. The incorporated adipose-derived stem cells (ADSCs) retained > 90% viable with proliferative capacity. In their latest updated *in vivo* work,<sup>40</sup> full-thickness chondral defects were created in a large animal (i.e., sheep) model, which were treated with the hand-held *in situ* bioprinted scaffold. The regenerated cartilage at 8 weeks after surgery showed better overall macroscopic and microscopic scores, and higher amount of neo-cartilage evidenced by COL-II expression, when compared with control groups (preconstructed 3D bioscaffolds, microfractures, and untreated controls).

Table 1 summarizes properties and biological outcomes of the fabricated constructs in these 27 presented studies.

### Considerations for Cartilage Bioprinting and Future Perspectives

Cartilage is a tissue that exhibits great heterogeneity and complex microarchitecture. Articular cartilage is comprised of three anatomic zones, namely the superficial zone, the middle zone and the deep zone.<sup>41</sup> The thin superficial zone occupies approximately 10% to 20% of articular cartilage thickness. The middle zone lies deep to the superficial zone, composing 40% to 60% of the total cartilage thickness, which contains proteoglycans and thicker collagen fibrils. The deep zone makes up approximately 30% of articular cartilage volume, in which collagen fibrils are arranged perpendicular to the articular surface. Separated by the tide mark, the deep zone is distinguished from the calcified cartilage, which plays an important role in transmitting from soft cartilage to bone.<sup>42</sup> Current clinical restorative technologies as well as TE strategies have been unable to recapitulate this complex microarchitecture and the resultant disorganized repair tissue is a major reason for failure of current basic science and clinical strategies.<sup>3</sup> Three-dimensional bioprinting has demonstrated the ability to reproduce chondral tissue with appropriate zonal structure owing to its capability of precise deposition of cells, biomaterials, growth factors, and other bioactive reagents to build cell-laden constructs.<sup>43</sup> This shows promise moving forward in clinical application of these 3D bioprinted constructs for *in vivo* articular cartilage restoration. Several of the studies included in this review demonstrate the ability to recapitulate the complex zonal microarchitecture of native hyaline cartilage as discussed in the “Bioprinting for Zonally Stratified Arrangement” section.

One of the principal functions of cartilage is to facilitate the transmission of loads. Engineered cartilage tissue ideally exhibits mechanical compressive strength which approaches to the value of native cartilage (e.g., compressive modulus: ~1.5 MPa<sup>37</sup>). Bioprinted cartilage tissue constructs have fallen short, demonstrating compressive moduli usually less than 100 kPa.<sup>15,18,20,28,33</sup> Researchers have strived to increase the mechanical properties by adjusting the concentration or chemical structure of the printed materials. Cui *et al.*<sup>27</sup> have doubled the concentration of PEGDMA (from 10% to 20%) to increase the compressive modulus nearly 10-fold (from ~40 to 400 kPa). Nevertheless, the enhanced mechanical properties remained insufficient for cartilage tissue engineering. In addition, there were concerns that the increased hydrogel concentration may hinder the cell proliferation and ECM formation.

Reinforcing the hydrogel carriers with synthetic polymers may serve as a method to reinforce their mechanical strength. PCL is one of the most popular biopolymers for engineering tissues due to its good elastomeric properties and high elasticity.<sup>44-46</sup> In addition to mechanical enhancement, it allows for the production of large constructs with high fidelity and fiber resolution.<sup>47,48</sup> Daly *et al.*<sup>14</sup> co-deposited hydrogel bioinks with fused PCL fibers. As compared to the hydrogel constructs with insufficient mechanical strength (~5-35 kPa), the PCL-reinforced hydrogel generated scaffolds had compressive moduli (~2 MPa) similar to that seen with native articular cartilage. PCL has shown to be a successful substrate in various heat distributions and concentrations while also having increased mechanical stability in highly stacked hydrogels.<sup>22,23,36</sup> One major concern of printing fused PCL fibers concurrently with cell-loaded hydrogel was that high temperature (e.g., 65°C to 80°C) was required to melt the PCL, which may decrease cell viability. Izadifar *et al.*<sup>23</sup> has monitored the surface temperature of the printed PCL fibers, and found that temperature dropped significantly once printed, and reached the values (e.g., 34°C to 39°C) that were suitable for cell survival. Other strategies to reinforce the constructs have been also proposed, such as employing electrospun PCL layers<sup>31</sup> or imbedding PLA microcarriers<sup>33</sup> in conjunction with cell-laden hydrogel.

Hydrogels have traditionally been used as a scaffold in bioprinting for a number of reasons including a decrease in the toxicity to the bioprinted cells as well as the increase in the biocompatibility of the constructs.<sup>49</sup> Scaffold-free bioprinting is a novel technique that may eliminate that need, which has been highlighted here.<sup>37</sup> Scaffold-free bioprinting offers relatively high initial cell density without the inclusion of biomaterials. This results in more space for ECM deposition, facilitates better cell-to-cell interactions, generates tissues with biomimicry, and preserves cell functionality with elimination of biodegradation issues.<sup>37,50</sup>

Chondrocytes and MSCs were the most common cell types used in the 27 studies. Chondrocytes are often difficult to obtain, whereas MSCs, which are more easily obtained, are capable of differentiating into both bone and cartilage cells.<sup>42</sup> It is well known that chondrocytes in different zones show distinct morphologies. The typical rounded shape of chondrocytes is found in the middle and deep zones, while the chondrocytes are more spread in the superficial zone.<sup>51</sup> Such morphological difference results in varied cellular activity in different zones of cartilage (e.g., ECM productions). Izadifar *et al.*<sup>23</sup> isolated chondrocytes with rounded and fibroblastic morphologies. A significantly higher expression of COL-II was observed within the rounded cells, while higher level of COL-I was found in the fibroblastic cells. Fibroblastic cells were similar to chondroprogenitors and act functionally like stem cells where rounded cells expressed prototypical chondrocyte morphology. These findings provide promising strategies for future bioprinted cartilage TE, which could incorporate multiple cell types into a zonal/stratified construct or guide the cells to generate proper morphologies and ECM productions. Steadily decrease of chondrocytes' redifferentiation capacity after several passages constrains their efficacy for TE of larger defects.<sup>34</sup> To overcome this limitation, multipotent progenitor cells, such as MSC and ADSCs have also been applied for various TE applications.<sup>52-54</sup> However, their tendency to undergo hypertrophic differentiation and trigger endochondral ossification remains a major concern.<sup>55</sup> Particularly, ACPCs were used in one of the abovementioned study,<sup>34</sup> which are capable of *in vitro* self-renewal, and can be expanded to > 60 passages while maintaining their potential in multilineage differentiation.<sup>56</sup> Moreover, different from MSCs, ACPCs showed resistance to formation of calcified tissue and hypertrophy, and maintained consistent production of hyaline-like cartilage.<sup>57,58</sup>

In addition to the selection of cell type, cell seeding density must also be taken into account. Ren *et al.*<sup>35</sup> printed hydrogels with different total cell density (i.e., 2, 1, and  $0.5 \times 10^7$  cells/mL). The group with cell density of  $1 \times 10^7$  cells/mL, which had a biomimetic cell density similar to native cartilage (10 million cells/mL<sup>59</sup>), demonstrated upregulated total GAG production and biosynthetic ability for single cell. Similarly, Cui *et al.*<sup>26</sup> used a low cell density of  $0.8 \times 10^7$  cells/mL and a high cell density of  $2 \times 10^7$  cells/mL. They found that ECM expression for single chondrocyte in low cell density was significantly greater than that in high cell density. Higher cell density demonstrated a more robust production of ECM. However, when evaluating the comparative ECM from individual chondrocytes, they produced more total ECM in lower density scenarios. This supports utilizing moderate cell density to maximize cell number and ECM production for an effectively engineered cartilage.<sup>22,27</sup> Constructs with elevated cell density may become metabolically quiescent due to limited nutrient

supply while those with low cell density may have limitations in cell-cell interactions. Manipulation of the cell density and distribution does provide a potential outlet for the generation of the zonal distribution of cells seen in native articular cartilage.<sup>22,27</sup>

During daily activity, articular cartilage is repeatedly subjected to forces generated by joint loading with varying frequencies between 0.1 and 10 Hz.<sup>60,61</sup> The transduction of mechanical signals stimulate changes in chondrocyte activity, such as metabolic events and structural adaptations.<sup>62,63</sup> The mechanical forces applied in the knee distribute stress within the articular zones in an asymmetrical pattern (e.g., high strain and shear stress in the superficial zone, small strain in lower and deep zones). Different ways of providing mechanical stresses have been reported, including unconfined uniaxial compression,<sup>64</sup> direct shear stress,<sup>65</sup> and hydrostatic pressure.<sup>66</sup> In development of bioprinted constructs, semi-confined compression, in which load was applied axially and rest of the construct is constrained is ideal, since it could closely mimic the native mechanical environment and resemble a gradient of the zones.<sup>67</sup> In future studies, this could be investigated with modulated mechanical environments into the culture, to give insights of how mechanical stimuli regulate the cell activities in the bioprinted constructs. Limitations of our study include the heterogeneous nature of the selected articles. Since cartilage bioprinting is still a novel topic, innovative studies are being produced every few years with new advances. Finally, the clinical translation is not yet clear and significantly more research is warranted before the techniques can be applied in clinics.

## Conclusion

Recent advances in bioprinting have granted cartilage TE the ability to assemble bioinks, cells, and signaling molecules into biologically relevant functional tissues. On screening the 360 articles based on PRISMA guidelines, the selected 27 studies have demonstrated 3D bioprinting of articular cartilage to be a TE strategy that has tremendous potential translational value. The unique abilities of the varied techniques including scaffold-based, scaffold-free and *in situ* bioprinting, have allowed replication of anatomical structure, biological function, and mechanical properties of the native articular cartilage, and particularly enabled the advances toward zonal differentiation, which have been proved by relatively comprehensive *in vitro* and *in vivo* studies. This review demonstrates that bioprinting has potential capacity for clinical cartilage reconstruction and future *in vivo* implantation as techniques are advanced.

## Acknowledgments and Funding

The author(s) received no financial support for the research, authorship, and/or publication of this article.

## Declaration of Conflicting Interests

The author(s) declared the following potential conflicts of interest with respect to the research, authorship, and/or publication of this article: Outside the submitted work NB has received money from the Pennsylvania Orthopedic Society and the American Academy of Orthopedic Surgeons. IO has stock/stock options in Biolife4D and Virtual Systems Engineering. AD has worked as a consultant and provided lectures for Smith & Nephew, has grants/grants pending for the Department of Defense, National Institute of Health, and Penn State University, and is an Arthroscopy Journal committee member/associate editor, part of AOSSM Publications Committee, Committee Member AANA Research Committee, Editorial Board OJSM, and Editorial Board SMAR.

## References

1. Bedi A, Feeley BT, Williams RJ 3rd. Management of articular cartilage defects of the knee. *J Bone Joint Surg Am*. 2010;92:994-1009.
2. Murawski CD, Kennedy JG. Operative treatment of osteochondral lesions of the talus. *J Bone Joint Surg Am*. 2013;95:1045-54.
3. Brittberg M, Lindahl A, Nilsson A, Ohlsson C, Isaksson O, Peterson L. Treatment of deep cartilage defects in the knee with autologous chondrocyte transplantation. *N Engl J Med*. 1994;331:889-95.
4. Peterson L, Vasiladis HS, Brittberg M, Lindahl A. Autologous chondrocyte implantation: a long-term follow-up. *Am J Sports Med*. 2010;38:1117-24.
5. Zhang YS, Yue K, Aleman J, Mollazadeh-Moghaddam K, Bakht SM, Yang J, *et al*. 3D bioprinting for tissue and organ fabrication. *Ann Biomed Eng*. 2017;45:148-63.
6. Mandrycky C, Wang Z, Kim K, Kim DH. 3D bioprinting for engineering complex tissues. *Biotechnol Adv*. 2016;34:422-34.
7. Dababneh AB, Ozbolat IT. Bioprinting technology: a current state-of-the-art review. *J Manuf Sci Eng*. 2014;136:061016.
8. Gudapati H, Dey M, Ozbolat I. A comprehensive review on droplet-based bioprinting: past, present and future. *Biomaterials*. 2016;102:20-42.
9. Ozbolat IT, Hospodiuk M. Current advances and future perspectives in extrusion-based bioprinting. *Biomaterials*. 2016;76:321-43.
10. Hospodiuk M, Moncal KK, Dey M, Ozbolat IT. Extrusion-based biofabrication in tissue engineering and regenerative medicine. In: Ovsianikov A, Yoo J and Mironov V editors. *3D printing and biofabrication*. Berlin, Germany: Springer; 2016. p. 1-27.
11. Bauge C, Boumediene K. Use of adult stem cells for cartilage tissue engineering: current status and future developments. *Stem Cells Int*. 2015;2015:438026.
12. Datta P, Barui A, Wu Y, Ozbolat V, Moncal KK, Ozbolat IT. Essential steps in bioprinting: from pre-to post-bioprinting. *Biotechnol Adv*. 2018;36:1481-504.
13. Peng W, Datta P, Wu Y, Dey M, Ayan B, Dababneh A, *et al*. Challenges in bio-fabrication of organoid cultures. *Adv Exp Med Biol*. Epub June 1, 2018.
14. Daly AC, Critchley SE, Rencsok EM, Kelly DJ. A comparison of different bioinks for 3D bioprinting of fibrocartilage and hyaline cartilage. *Biofabrication*. 2016;8:045002.
15. Costantini M, Idaszek J, Szoke K, Jaroszewicz J, Dentini M, Barbetta A, *et al*. 3D bioprinting of BM-MSCs-loaded ECM biomimetic hydrogels for in vitro neocartilage formation. *Biofabrication*. 2016;8:035002.
16. Mouser VH, Melchels FP, Visser J, Dhert WJ, Gawlitta D, Malda J. Yield stress determines bioprintability of hydrogels based on gelatin-methacryloyl and gellan gum for cartilage bioprinting. *Biofabrication*. 2016;8:035003.
17. Abbadessa A, Mouser VHM, Blokzijl MM, Gawlitta D, Dhert WJA, Hennink WE, *et al*. A synthetic thermosensitive hydrogel for cartilage bioprinting and its biofunctionalization with polysaccharides. *Biomacromolecules*. 2016;17:2137-47.
18. Abbadessa A, Blokzijl MM, Mouser VH, Marica P, Malda J, Hennink WE, *et al*. A thermo-responsive and photo-polymerizable chondroitin sulfate-based hydrogel for 3D printing applications. *Carbohydr Polym*. 2016;149:163-74.
19. Mouser VHM, Abbadessa A, Levato R, Hennink WE, Vermonden T, Gawlitta D, *et al*. Development of a thermosensitive HAMA-containing bio-ink for the fabrication of composite cartilage repair constructs. *Biofabrication*. 2017;9:015026.
20. Markstedt K, Mantas A, Tournier I, Martinez Avila H, Hagg D, Gatenholm P. 3D bioprinting human chondrocytes with nanocellulose-alginate bioink for cartilage tissue engineering applications. *Biomacromolecules*. 2015;16:1489-96.
21. Nguyen D, Hägg DA, Forsman A, Ekholm J, Nimkingratana P, Brantsing C, *et al*. Cartilage tissue engineering by the 3D bioprinting of iPS cells in a nanocellulose/alginate bioink. *Sci Rep*. 2017;7:658.
22. Kundu J, Shim JH, Jang J, Kim SW, Cho DW. An additive manufacturing-based PCL-alginate-chondrocyte bioprinted scaffold for cartilage tissue engineering. *J Tissue Eng Regen Med*. 2015;9:1286-97.
23. Izadifar Z, Chang T, Kulyk W, Chen X, Eames BF. Analyzing biological performance of 3D-printed, cell-impregnated hybrid constructs for cartilage tissue engineering. *Tissue Eng Part C Methods*. 2016;22:173-88.
24. Olubamiji AD, Zhu N, Chang T, Nwankwo CK, Izadifar Z, Honaramooz A, *et al*. Traditional invasive and synchrotron-based noninvasive assessments of three-dimensional-printed hybrid cartilage constructs in situ. *Tissue Eng Part C Methods*. 2017;23:156-68.
25. Yang X, Lu Z, Wu H, Li W, Zheng L, Zhao J. Collagen-alginate as bioink for three-dimensional (3D) cell printing based cartilage tissue engineering. *Mater Sci Eng C*. 2018;83:195-201.
26. Cui X, Breitenkamp K, Finn MG, Lotz M, D'Lima DD. Direct human cartilage repair using three-dimensional bioprinting technology. *Tissue Eng Part A*. 2012;18:1304-12.
27. Cui X, Breitenkamp K, Lotz M, D'Lima D. Synergistic action of fibroblast growth factor-2 and transforming growth factor-beta1 enhances bioprinted human neocartilage formation. *Biotechnol Bioeng*. 2012;109:2357-68.

28. Gao G, Yonezawa T, Hubbell K, Dai G, Cui X. Inkjet-bioprinted acrylated peptides and PEG hydrogel with human mesenchymal stem cells promote robust bone and cartilage formation with minimal printhead clogging. *Biotechnol J*. 2015;10:1568-77.
29. Gao G, Schilling AF, Hubbell K, Yonezawa T, Truong D, Hong Y, *et al.* Improved properties of bone and cartilage tissue from 3D inkjet-bioprinted human mesenchymal stem cells by simultaneous deposition and photocrosslinking in PEG-GelMA. *Biotechnol Lett*. 2015;37:2349-55.
30. Gao G, Zhang XF, Hubbell K, Cui X. NR2F2 regulates chondrogenesis of human mesenchymal stem cells in bioprinted cartilage. *Biotechnol Bioeng*. 2017;114:208-16.
31. Xu T, Binder KW, Albanna MZ, Dice D, Zhao W, Yoo JJ, *et al.* Hybrid printing of mechanically and biologically improved constructs for cartilage tissue engineering applications. *Biofabrication*. 2013;5:015001.
32. Zhu W, Cui H, Boualam B, Masood F, Flynn E, Rao RD, *et al.* 3D bioprinting mesenchymal stem cell-laden construct with core-shell nanospheres for cartilage tissue engineering. *Nanotechnology*. 2018;29:185101.
33. Levato R, Visser J, Planell JA, Engel E, Malda J, Mateos-Timoneda MA. Biofabrication of tissue constructs by 3D bioprinting of cell-laden microcarriers. *Biofabrication*. 2014;6:035020.
34. Levato R, Webb WR, Otto IA, Mensinga A, Zhang Y, van Rijen M, *et al.* The bio in the ink: cartilage regeneration with bioprintable hydrogels and articular cartilage-derived progenitor cells. *Acta Biomater*. 2017;61:41-53.
35. Ren X, Wang F, Chen C, Gong X, Yin L, Yang L. Engineering zonal cartilage through bioprinting collagen type II hydrogel constructs with biomimetic chondrocyte density gradient. *BMC Musculoskelet Disord*. 2016;17:301.
36. Shim JH, Jang KM, Hahn SK, Park JY, Jung H, Oh K, *et al.* Three-dimensional bioprinting of multilayered constructs containing human mesenchymal stromal cells for osteochondral tissue regeneration in the rabbit knee joint. *Biofabrication*. 2016;8:014102.
37. Yu Y, Moncal KK, Li J, Peng W, Rivero I, Martin JA, *et al.* Three-dimensional bioprinting using self-assembling scalable scaffold-free "tissue strands" as a new bioink. *Sci Rep*. 2016;6:28714.
38. O'Connell CD, Di Bella C, Thompson F, Augustine C, Beirne S, Cornock R, *et al.* Development of the Biopen: a handheld device for surgical printing of adipose stem cells at a chondral wound site. *Biofabrication*. 2016;8:015019.
39. Duchi S, Onofrillo C, O'Connell CD, Blanchard R, Augustine C, Quigley AF, *et al.* Handheld co-axial bioprinting: application to in situ surgical cartilage repair. *Sci Rep*. 2017;7:5837.
40. Di Bella C, Duchi S, O'Connell CD, Blanchard R, Augustine C, Yue Z, *et al.* In situ handheld three-dimensional bioprinting for cartilage regeneration. *J Tissue Eng Regen Med*. 2018;12:611-21.
41. Fox AJS, Bedi A, Rodeo SA. The basic science of articular cartilage: structure, composition, and function. *Sports Health*. 2009;1:461-8.
42. Temenoff JS, Mikos AG. Review: tissue engineering for regeneration of articular cartilage. *Biomaterials*. 2000;21:431-40.
43. Hospodiuk M, Dey M, Sosnoski D, Ozbolat IT. The bioink: a comprehensive review on bioprintable materials. *Biotechnol Adv*. 2017;35:217-39.
44. Woodruff MA, Hutmacher DW. The return of a forgotten polymer-polycaprolactone in the 21st century. *Prog Polym Sci*. 2010;35:1217-56.
45. Wu Y, Wang Z, Fuh JYH, San Wong Y, Wang W, Thian ES. Mechanically-enhanced three-dimensional scaffold with anisotropic morphology for tendon regeneration. *J Mater Sci Mater Med*. 2016;27:115.
46. Wu Y, Sriram G, Fawzy AS, Fuh JY, Rosa V, Cao T, *et al.* Fabrication and evaluation of electrohydrodynamic jet 3D printed polycaprolactone/chitosan cell carriers using human embryonic stem cell-derived fibroblasts. *J Biomater Appl*. 2016;31:181-92.
47. Lee CH, Rodeo SA, Fortier LA, Lu C, Erisken C, Mao JJ. Protein-releasing polymeric scaffolds induce fibrochondrocytic differentiation of endogenous cells for knee meniscus regeneration in sheep. *Sci Transl Med*. 2014;6:266ra171.
48. Ding C, Qiao Z, Jiang W, Li H, Wei J, Zhou G, *et al.* Regeneration of a goat femoral head using a tissue-specific, biphasic scaffold fabricated with CAD/CAM technology. *Biomaterials*. 2013;34:6706-16.
49. Reichert JC, Heymer A, Berner A, Eulert J, Noth U. Fabrication of polycaprolactone collagen hydrogel constructs seeded with mesenchymal stem cells for bone regeneration. *Biomed Mater*. 2009;4:065001.
50. Ozbolat IT. Scaffold-based or scaffold-free bioprinting: competing or complementing approaches? *J Nanotechnol Eng Med*. 2015;6:024701.
51. Panadero J, Lanceros-Mendez S, Ribelles JG. Differentiation of mesenchymal stem cells for cartilage tissue engineering: individual and synergetic effects of three-dimensional environment and mechanical loading. *Acta Biomater*. 2016;33:1-12.
52. Guo X, Park H, Young S, Kretlow JD, Van den Beucken JJ, Baggett LS, *et al.* Repair of osteochondral defects with biodegradable hydrogel composites encapsulating marrow mesenchymal stem cells in a rabbit model. *Acta Biomater*. 2010;6:39-47.
53. Wu Y, Han Y, Wong YS, Fuh JYH. Fiber-based scaffolding techniques for tendon tissue engineering. *J Tissue Eng Regen Med*. 2018;12:1798-821.
54. Park JS, Shim MS, Shim SH, Yang HN, Jeon SY, Woo DG, *et al.* Chondrogenic potential of stem cells derived from amniotic fluid, adipose tissue, or bone marrow encapsulated in fibrin gels containing TGF- $\beta$ 3. *Biomaterials*. 2011;32:8139-49.
55. Visser J, Gawlitta D, Benders KE, Toma SM, Pouran B, van Weeren PR, *et al.* Endochondral bone formation in gelatin methacrylamide hydrogel with embedded cartilage-derived matrix particles. *Biomaterials*. 2015;37:174-82.
56. Williams R, Khan IM, Richardson K, Nelson L, McCarthy HE, Anabalsi T, *et al.* Identification and clonal characterization of a progenitor cell sub-population in normal human articular cartilage. *PLoS One*. 2010;5:e13246.
57. McCarthy HE, Bara JJ, Brakspear K, Singhrao SK, Archer CW. The comparison of equine articular cartilage progenitor cells



- and bone marrow-derived stromal cells as potential cell sources for cartilage repair in the horse. *Vet J.* 2012;192:345-51.
58. Neumann AJ, Gardner OF, Williams R, Alini M, Archer CW, Stoddart MJ. Human articular cartilage progenitor cells are responsive to mechanical stimulation and adenoviral-mediated overexpression of bone-morphogenetic protein 2. *PLoS One.* 2015;10:e0136229.
  59. Hunziker EB, Quinn TM, Häuselmann HJ. Quantitative structural organization of normal adult human articular cartilage. *Osteoarthr Cartil.* 2002;10:564-72.
  60. Van Kampen GPJ, Veldhuijzen JP, Kuijjer R, Van de Stadt RJ, Schipper CA. Cartilage response to mechanical force in high-density chondrocyte cultures. *Arthritis Rheum.* 1985;28:419.
  61. Elder BD, Athanasiou KA. Hydrostatic pressure in articular cartilage tissue engineering: from chondrocytes to tissue regeneration. *Tissue Eng Part B Rev.* 2009;15:43-53.
  62. Sah LY, Kim YJ, Doong JYH, Grodzinsky AJ, Plass AHK, Sandy JD. Biosynthetic response of cartilage explants to dynamic compression. *J Orthop Res.* 1989;7:619-36.
  63. Salter RB, Simmonds DF, Malcolm BW, Rumble EJ, Macmichael D, Clements ND. The biological effect of continuous passive motion on the healing of full-thickness defects in articular cartilage. An experimental investigation in the rabbit. *J Bone Joint Surg Am.* 1981;68:1232-51.
  64. Huang AH, Farrell MJ, Kim M, Mauck RL. Long-term dynamic loading improves the mechanical properties of chondrogenic mesenchymal stem cell-laden hydrogels. *Eur Cell Mater.* 2010;19:72-85.
  65. Li Z, Yao SJ, Alini M, Stoddart MJ. Chondrogenesis of human bone marrow mesenchymal stem cells in fibrin-polyurethane composites is modulated by frequency and amplitude of dynamic compression and shear stress. *Tissue Eng Part A.* 2009;16:575-84.
  66. Miyashita K, Trindade MC, Lindsey DP, Beaupré GS, Carter DR, Goodman SB, *et al.* Effects of hydrostatic pressure and transforming growth factor- $\beta$  3 on adult human mesenchymal stem cell chondrogenesis in vitro. *Tissue Eng.* 2006;12:1419-28.
  67. Thorpe SD, Nagel T, Carroll SF, Kelly DJ. Modulating gradients in regulatory signals within mesenchymal stem cell seeded hydrogels: a novel strategy to engineer zonal articular cartilage. *PLoS One.* 2013;8:e60764.
  68. Ozbolat IT. 3D bioprinting: fundamentals, principles and applications. San Diego, CA: Academic Press; 2016.